

Reinvestigating the R2 Indicator

Achieving Pareto Compliance by Integration

Lennart Schäpermeier^[0000–0003–3929–7465] and
Pascal Kerschke^[0000–0003–2862–1418]

Big Data Analytics in Transportation, TU Dresden, Germany &
ScaDS.AI Dresden/Leipzig, Germany

{lennart.schaepermeier,pascal.kerschke}@tu-dresden.de

Abstract. In multi-objective optimization, set-based quality indicators are a cornerstone of benchmarking and performance assessment. They capture the quality of a set of trade-off solutions by reducing it to a scalar number. One of the most commonly used set-based metrics is the R2 indicator, which describes the expected utility of a solution set to a decision-maker under a distribution of utility functions. Typically, this indicator is applied by discretizing this distribution of utility functions, yielding a weakly Pareto-compliant indicator. In consequence, adding a nondominated or dominating solution to a solution set *may* – but does not have to – improve the indicator’s value.

In this paper, we reinvestigate the R2 indicator under the premise that we have a continuous, uniform distribution of (Tchebycheff) utility functions. We analyze its properties in detail, demonstrating that this continuous variant is indeed Pareto-compliant – that is, any beneficial solution will improve the metric’s value. Additionally, we provide an efficient computational procedure to compute this metric for bi-objective problems in $\mathcal{O}(N \log N)$. As a result, this work contributes to the state-of-the-art Pareto-compliant unary performance metrics, such as the hypervolume indicator, offering an efficient and promising alternative.

Keywords: Performance assessment · Multi-objective optimization · R2 indicator · Benchmarking · Utility functions · Pareto compliance.

1 Introduction

When optimizing any system, there is often not just one objective, but multiple criteria required to assess the quality of a solution. Rather than aggregating these different optimization objectives into one, e.g., by means of a linear combination of the individual objectives, the domain of multi-objective (MO) optimization aims to find a set of (Pareto-)optimal trade-off solutions to present to a decision-maker [13]. However, to benchmark MO optimizers and facilitate algorithm design, parameter tuning, and automated algorithm selection, quantifying the quality of trade-off solutions in a unary set-based performance indicator is often necessary.

To be reasonably interpretable, it is recommended that a MO performance indicator fulfills a property that is known as Pareto compliance [8]. More precisely, a set-based performance indicator is called Pareto-compliant, if and only if its indicator value for set A is better than for set B when set A dominates set B. In addition, an indicator is called weakly Pareto-compliant if its value for set A is not worse than for set B.

Up to now, the hypervolume (HV) indicator, and variants thereof, are the only set-based performance indicators that are recognized as truly Pareto-compliant [17,2,9]. The HV indicator computes the m -dimensional hypervolume dominated by the solution set w.r.t. to a user-specified anti-optimal reference point.

In contrast, there are multiple families of weakly Pareto-compliant indicators. Exemplary and widely used representatives are the IGD+ indicator [11], requiring an (approximated or known) reference Pareto front, or the R2 indicator [10,5], requiring an ideal/utopian reference point as well as a sample of aggregation (or: utility) functions.

The R2 indicator, in particular, may be an attractive choice as it requires an ideal rather than an anti-optimal reference point. In many problems, the ideal point is easier to find, e.g., in multi-objective machine learning problems where optimal, but not always anti-optimal, values for loss functions are available. Also, solutions that do not dominate a chosen reference point may not contribute to the dominated hypervolume, and a reference point far away from the Pareto front (PF) tends to put a high weight on solutions at the PF’s boundary, which is also often undesirable. Another benefit arises when constructing test problems from objectives with known single-objective optima, which lack a natural upper bound for the reference point or a clear “region of interest”.

While the unary R2 indicator was initially defined as an integral over a continuum of utility functions by [10], it is usually only discussed and applied in an approximate manner for which the distribution of utility functions is discretized [5,14]. The latter comes with the benefit of being flexible regarding the involved utility functions. It also provides a convenient way to compute the indicator as an average of multiple utility functions, however, sacrificing Pareto compliance in the process. In this paper, we consider the most common R2 indicator definition with a uniform distribution of Tchebycheff utility functions [10,5]. Our main contribution is the methodology to compute this indicator exactly for a set of solutions in the bi-objective case, thereby preserving its Pareto compliance. We achieve this by shifting perspective away from averaging over predefined utility functions towards computing the R2 indicator contributions of each individual nondominated point, thereby eliminating weaknesses in the R2 indicator’s properties. Additionally, we demonstrate the exact R2 indicator values for individual points and linear Pareto fronts, as well as the approximate nature of the discretization-based approach commonly used so far.

This paper is structured as follows: We introduce multi-objective optimization and set-based performance assessment in Section 2. Then, in Section 3, we derive the methodology for computing exact R2 indicator values, first for a single solution and then for a set of solutions. Section 4 presents some exemplary re-

sults regarding characteristics of the exact R2 indicator, and Section 5 concludes the paper with an outlook on future research avenues.

2 Background

We begin by introducing some fundamental aspects of multi-objective optimization and dominance relationships of multi-objective solutions. Then, we will cover core aspects of set-based performance assessment in multi-objective optimization and its best known representative, the hypervolume indicator. Finally, we introduce the R2 indicator with its most important properties for the discretized and the exact variant.

2.1 Multi-objective Optimization

In multi-objective (MO) optimization, we aim to (w.l.o.g.) minimize multiple conflicting objectives. Commonly, a MO optimization problem (MOP) with m objectives is given by an objective function $F : \mathcal{X} \mapsto \mathbb{R}^m$ where \mathcal{X} represents the decision space. The individual objectives are denoted as $f_i : \mathcal{X} \mapsto \mathbb{R}, i = 1, \dots, m$ in this work. Further, we are primarily considering the bi-objective setting ($m = 2$). Depending on the particular problem and decision space, there may be further constraints on admissible solutions.

A particular challenge posed by MOPs pertains to solution comparison. While in single-objective optimization, solutions can be compared directly (either they have identical objective values or one is better than another), such immediate comparisons are not possible for all solutions of a MOP. To solve this, we need the concept of dominance. A solution x *dominates* another solution y ($x \prec y$), iff $f_i(x) \leq f_i(y)$ for all i and $f_i(x) < f_i(y)$ for at least one i . A solution x *strongly dominates* another solution y if the stronger condition $f_i(x) < f_i(y)$ holds for all i . A solution that dominates, but does not strongly dominate, another solution is also called *weakly dominant*. Finally, two solutions can be incomparable, that is, *mutually nondominated*, if either fulfills some objective better than the other.

Definitions of dominance can also be extended to sets of solutions. A set of solutions A (weakly) dominates another set B , if each member of B is (weakly) dominated by a solution in A , written as $A \preceq B$ and $A \prec B$, respectively [18,8].

The set of all nondominated solutions $P = \{x \in \mathcal{X} \mid \nexists y \in \mathcal{X} : y \prec x\}$ is known as the Pareto set, and its image under F is known as the Pareto front. The Pareto set contains the optimal trade-off solutions regarding the objectives, and aiming to obtain a close approximation to it is the prevalent approach of solving MOPs when no further constraints or preferences on the objectives are known, i.e., under black-box assumptions. Evolutionary algorithms are the most widespread approach for finding good Pareto set approximations in these conditions.

Finally, we call the vector of the optimal, individual function values *ideal point*, and refer to the best vector dominated by all Pareto optimal points as *nadir point*. Often, before computing indicator values and if the ideal and nadir points are available, the region between them is normalized to the $[0, 1]^m$ box in objective space as a normalization technique.

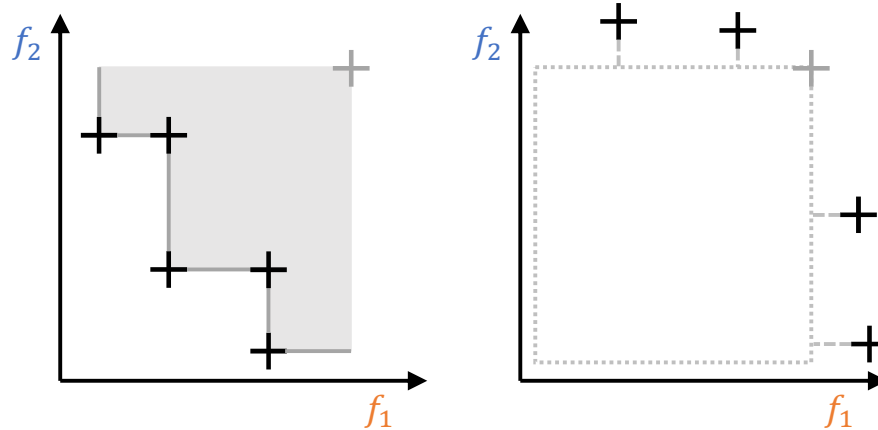


Fig. 1. Left: Illustration of the HV indicator. Right: If no point dominating the HV is found, the minimal distance to the region of interest (dotted) can be used as an additional indicator. The combined indicator is, however, not Pareto-compliant anymore.

2.2 Set-based Performance Assessment

As the Pareto set generally contains more than one solution, set-based performance measures are the norm in assessing the overall quality of an archive of evaluated points. This need to quantify Pareto set approximations has led to numerous performance measures being introduced. For a recent survey on MO performance indicators, we refer to [1].

The most prominent set-based performance measure is the dominated hypervolume (HV) indicator (or: S -metric) that measures the space dominated by the set of solutions w.r.t. an anti-optimal reference point [17,2,9]. An illustration of the HV indicator for two objectives is given in Figure 1.

An important property of a set-based performance measure $I : \mathbb{R}^m \rightarrow \mathbb{R}$ is *Pareto compliance*: If $A \preceq B$ and $B \not\preceq A$, then $I(A) < I(B)$ [18]. That is, a performance measure should improve if new non-dominated or (weakly) dominating solutions are added to a set of solutions. If only $I(A) \leq I(B)$ can be guaranteed under the same circumstances, I is called *weakly Pareto-compliant*. Only the HV indicator and other indicators based on it are established to be Pareto-compliant [9]. The selection of weakly Pareto-compliant indicators is somewhat larger, including, for example, the (discretized) R2 [5] and the IGD+ [11] measures.

The necessity of the anti-optimal reference point can, however, be a hindrance to achieving Pareto compliance in practice. Setting the reference point so far back that it is dominated by every feasible solution introduces a bias towards the edges of the PF, while a reference point close to the nadir point fails to consider all solutions outside of such a defined region of interest, cf. Figure 1.

2.3 The R2 Indicator

In contrast to the HV indicator, the unary R2 indicator is ordinarily defined as the expected utility of the point set w.r.t. a distribution of utility functions U [10]. In the most general case, for a set of solutions Y of a MOP, we can define it as follows:

$$R2(Y) := \int_{u \in U} \min_{y \in Y} u(y) du.$$

The most common choice of a utility function is a Tchebycheff aggregation, which allows to reach all Pareto-optimal points depending on the chosen parametrization. For a weight vector $w \in [0, 1]^m$ with $\sum_{i=1}^m w_i = 1$ and a utopian vector y^* , it is given by

$$\begin{aligned} u_w(y) &= \max_{i=1, \dots, m} w_i (y_i - y_i^*) \\ &= \max_{i=1, \dots, m} w_i y'_i \end{aligned}$$

using $y'_i = y_i - y_i^*$ to shift the utopian point w.l.o.g. to the origin. The distribution of utility functions is then usually chosen as uniform on the weight simplex.

In the bi-objective case, where $w_2 = w_1 - 1$ holds, this yields the following formula for $R2$:

$$\begin{aligned} R2(Y) &= \int_0^1 \min_{y \in Y} u_w(Y) dw \\ &= \int_0^1 \min_{y \in Y} \{\max(wy'_1, (1-w)y'_2)\} dw. \end{aligned}$$

As there is no apparent way to calculate this property directly, it is generally approximated in a discrete manner by discretizing U using $n = |W|$ weight vectors $w \in W$:

$$R2(Y) \approx \frac{1}{|W|} \sum_{w \in W} \min_{y \in Y} u_w(y).$$

As an example, the uniform weight distribution with size n for the bi-objective case is given by [5]

$$W = \left\{ (0, 1), \left(\frac{1}{n-1}, \frac{n-2}{n-1} \right), \dots, \left(\frac{n-2}{n-1}, \frac{1}{n-1} \right), (1, 0) \right\}.$$

The discretization is simultaneously a blessing and a curse: On the one hand, it provides an effective method of approximating the underlying exact $R2$ value with high precision. On the other hand, this weakens the indicators' properties. To optimize the discretized R2 indicator, one can consider at most $|W|$ points on the Pareto front, which optimize u_w for each $w \in W$, respectively. Additional nondominated solutions cannot contribute to the indicator value. Further, an individual utility function u_w may be optimized by a point that is only weakly

Pareto optimal, but has the same utility (for this set of weights) as another, Pareto optimal point. See, for example, the top left image of Figure 2, where each point along the vertical lines would have identical utility values. This places the discretized R2 indicator among the weakly Pareto-compliant indicators.

A final property of the R2 indicator is that each solution y from a nondominated set of solutions Y is optimal in terms of utility compared to all other solutions from Y for a particular weight $(w^*, 1 - w^*)$ such that [5]

$$\begin{aligned} w^* y'_1 &= (1 - w^*) y'_2 \\ \Rightarrow w^* &= \frac{y'_2}{y'_1 + y'_2}. \end{aligned}$$

Discussions around the R2 indicator and its application focus (almost) exclusively on its discrete variant [5,16] rather than on the original continuous definition of R2 [10]. The remainder of this paper is dedicated to a better understanding of this original definition, analyzing its properties, and detailing methods for computing it.

3 The R2 Indicator for Continuous Utility Distributions

In this section, we derive how the R2 indicator can be computed under the assumption of a continuous distribution of Tchebycheff utility functions for bi-objective problems. We will start by analyzing the scenario for a single solution point before extending the analysis to sets of solutions. At last, we derive the computational complexity of the presented approach.

3.1 R2 for a Single Solution

Without loss of generality, let $y^* = (0, 0)$ be the utopian point and $Y = \{y\}$ be the set containing only one solution $y = (y_1, y_2) > (0, 0)$. Further, let $w = (w^*, 1 - w^*)$ be the weight vector such that $w^* y_1 = (1 - w^*) y_2$. Then, for $w_1 < w^*$, $w_1 y_1 < (1 - w_1) y_2$ and for $w_1 > w^*$, $w_1 y_1 > (1 - w_1) y_2$. Based on this observation, we can compute the exact R2 indicator of Y for a uniform distribution of Tchebycheff utility functions by splitting the integral along w^* :

$$\begin{aligned} R2(Y) &= \int_0^1 \max(y_1 w, y_2 (1 - w)) dw \\ &= \int_0^{w^*} y_2 (1 - w) dw + \int_{w^*}^1 y_1 w dw \\ &= \left[-\frac{1}{2} y_2 (1 - w)^2 \right]_0^{w^*} + \left[\frac{1}{2} y_1 w^2 \right]_{w^*}^1 \\ &= \frac{1}{2} y_2 (1 - (1 - w^*)^2) + \frac{1}{2} y_1 (1 - (w^*)^2). \end{aligned}$$

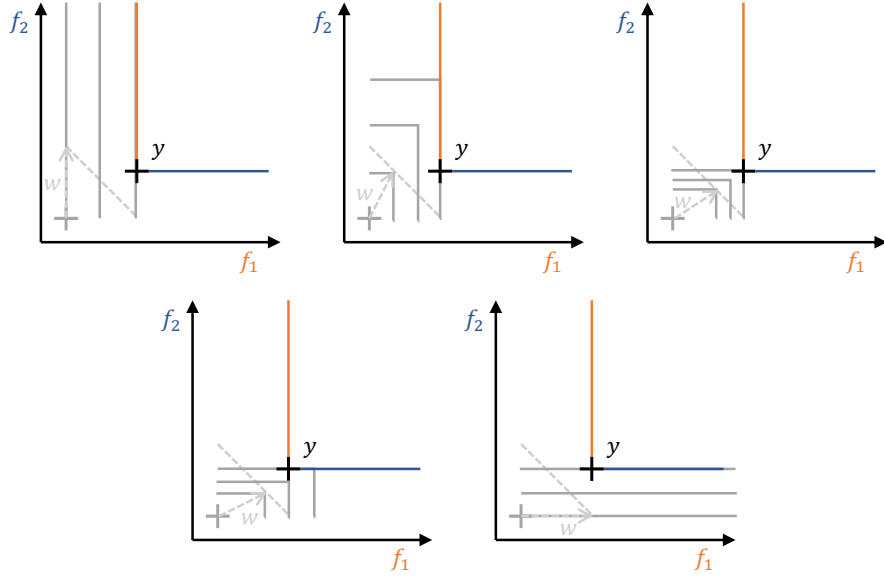


Fig. 2. Illustration of level sets of the Tchebycheff utility for five different weight vectors w . The utility value $u_w(y)$ is determined by the surface that the level set touches first: At vertical surfaces (see left and center image in the top row), the $u_w(y)$ is determined by the f_1 value while at horizontal surfaces (see bottom row) $u_w(y)$ depends on the f_2 value of y . At y (the top right figure) both $w_1 y_1$ and $w_2 y_2$ are identical. Note: Weight vectors are illustrated to point towards their equilibrium between both objectives, i.e., $w_1 f_1 = w_2 f_2$.

This simple case demonstrates that computing the exact R2 indicator for a set of solutions consists of the following steps: First, we need to identify areas in which the utility value does not vary w.r.t. y and is only sensitive to w . Then, we compute the contribution of each of these areas to the final R2 value using the corresponding integral and finally sum everything up.

We can build on these observations to derive a general procedure to compute $R2(Y)$ for arbitrary solution sets.

3.2 R2 for a Set of Solutions

Let us now consider what happens when our solution set contains $N > 1$ solutions. Let $Y = \{y^{(1)}, \dots, y^{(N)}\}$ be the set of *nondominated* solutions ordered by ascending y_1 value. Analogous to w^* above, let $w^{(n)} = (w_1^{(n)}, 1 - w_1^{(n)})$ be the weight vector such that $w_1^{(n)} y_1^{(n)} = (1 - w_1^{(n)}) y_2^{(n)}$ for all $n = 1, \dots, N$.

The weights $w^{(n)}$ indicate when the utility of solution $y^{(n)}$ is optimal and identical w.r.t. both individual objectives. Slightly increasing (decreasing) $w_1^{(n)}$ lets the term of the first (second) objective dominate, i.e., the $w^{(n)}$ values indicate a switch in the relevant objective.

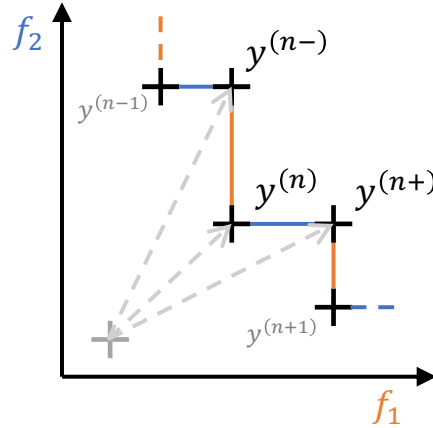


Fig. 3. Schematic illustration of the integration ranges of a solution $y^{(n)}$. $y^{(n-1)}$, $y^{(n)}$, and $y^{(n+1)}$ are consecutive points in the solution set. $y^{(n-)}$ and $y^{(n+)}$ correspond to the corners in the PF that are adjacent to $y^{(n)}$. Their corresponding weight vectors $w^{(n-)}$ and $w^{(n+)}$ indicate the boundaries in which $y^{(n)}$ locally determines the PF. At $w^{(n)}$, the objective switches between the f_1 - (vertical PF segment) and f_2 -values (horizontal PF segment) of solution $y^{(n)}$.

In addition, we need to identify the weight ranges for which the utility value is determined by a given solution $y^{(n)}$ rather than by one of its adjacent non-dominated solutions, $y^{(n-1)}$ or $y^{(n+1)}$. As a visual aid for the following explanations, Figure 3 provides a sketch of the involved solutions, weight vectors, and their relationships. For this purpose, let $w^{(n+)}$ be the weight vector such that $w_1^{(n+)}y_1^{(n+1)} = (1 - w_1^{(n+)})y_2^{(n)}$. $w^{(n+)}$ represents the weight vector pointing to the intersection between $y^{(n)}$ and $y^{(n+1)}$, marked as $y^{(n+)}$ in Figure 3, where the relevant solution switches between the two solution vectors. On the other side, $w^{(n-)}$ analogously defines the boundary between $y^{(n-1)}$ and $y^{(n)}$, which is indicated by $y^{(n-)}$ in Figure 3. Given these definitions, a solution $y^{(n)} = (y_1^{(n)}, y_2^{(n)})$ determines the Tchebycheff utility in the interval $[w_1^{(n-)}, w_1^{(n+)}]$ for w_1 , with the subinterval $[w_1^{(n-)}, w_1^{(n)}]$ being dependent on the y_2 -value and $[w_1^{(n)}, w_1^{(n+)}]$ depending on its y_1 -value.

Note also that, similarly to the HV indicator, the solution $y^{(n)}$ has an exclusive contribution corresponding to the box spanned by it with $y^{(n-)}$ and $y^{(n+)}$: The utilities $u_{w^{(n-)}} to $u_{w^{(n+)}}$ would worsen if $y^{(n)}$ was removed. This will still be true if we consider the case that $y^{(n)}$ would only weakly dominate one of its neighbors in the set, re-establishing Pareto compliance for the R2 indicator as it was described in its original publication [10].$

Now we can compute the partial R2 contribution of $y^{(n)}$ in a similar way to the single solution set by splitting along $w_1^{(n)}$. It only differs by replacing the overall integration boundaries by $y^{(n)}$'s relevant weight range, $w_1^{(n-)}$ and $w_1^{(n+)}$,

which gives:

$$\begin{aligned}
R2(y^{(n)}) &= \int_{w_1^{(n-)}}^{w_1^{(n+)}} \max(y_1^{(n)}w, y_2^{(n)}(1-w))dw \\
&= \int_{w_1^{(n-)}}^{w_1^{(n)}} y_2^{(n)}(1-w)dw + \int_{w_1^{(n)}}^{w_1^{(n+)}} y_1^{(n)}wdw \\
&= \left[-\frac{1}{2}y_2^{(n)}(1-w)^2 \right]_{w_1^{(n-)}}^{w_1^{(n)}} + \left[\frac{1}{2}y_1^{(n)}w^2 \right]_{w_1^{(n)}}^{w_1^{(n+)}} \\
&= \frac{1}{2}y_2^{(n)} \left((1-w_1^{(n-)})^2 - (1-w_1^{(n)})^2 \right) + \frac{1}{2}y_1^{(n)} \left((w_1^{(n+)})^2 - (w_1^{(n)})^2 \right).
\end{aligned}$$

For the special cases that $n = 1$ or $n = N$, where there is no neighbor in one direction, we can define $w_1^{(1-)} = 0$ and $w_1^{(N+)} = 1$, respectively.

Given the individual contributions $R2(y^{(n)})$ for all $n = 1, \dots, N$, we can construct the exact $R2$ value of the whole solution set Y simply as their sum:

$$R2(Y) = \sum_{n=1}^N R2(y^{(n)}).$$

In consequence, computing the exact $R2$ indicator for two objectives can essentially be achieved with a single pass along the N solutions from Y , as will be described next.

3.3 Computational Complexity

The computational complexity of this approach is determined mostly by the condition that we require Y to contain only nondominated solutions and be sorted by y_1 . For this, we can first sort an archive of solutions (including dominated points) by y_1 and pass over this list once, removing any dominated points and duplicates. This takes $\mathcal{O}(N \log N)$ time with standard sorting algorithms.

The computation of the indicator itself is then just a matter of another pass over the sorted list of nondominated points, which requires linear time: All required w and y values can be obtained on the fly based on any given point $y^{(n)}$ and its immediate neighbors. To summarize, the computation of the exact $R2$ indicator on an archive of N points in bi-objective space requires a complexity of $\mathcal{O}(N \log N)$. This improves upon the $\mathcal{O}(N|W|)$ complexity of the discretized $R2$ for precise indicator values and large sets of solutions, i.e., large $|W|$ and N values.

4 Properties of the Exact $R2$ Indicator

In this section, we present some empirical and theoretical results on our proposed exact $R2$ indicator. We start by demonstrating the approximation behaviour of

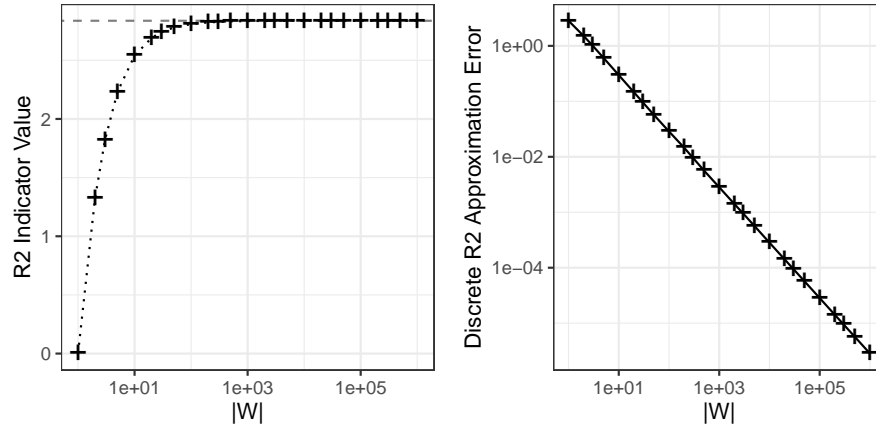


Fig. 4. Comparison of the approximated R2 indicator values using $|W|$ weight vectors and the exact R2 indicator value computed by our methodology. Left: The exact value is shown by the dashed line. Right: The corresponding approximation error of the discretized approach. The test set of solutions is given by 10^5 randomly evaluated points on a bi-sphere problem from the bi-objective BBOB [4] with parameters {FID: 1, IID: 1, DIM: 2}.

the discrete R2 in relation to the exact computation described in the previous sections. Then, we will calculate the optimal R2 indicator values for simple front shapes and demonstrate the convergence behaviour of the indicator w.r.t. increasingly large nondominated sets.

We implemented the exact R2 indicator in the statistical software R. For computations of the discrete R2 indicator, we utilize the `unary_r2_indicator` function from the `emoa` package [12]. The scripts to reproduce these experimental results are published at <https://github.com/schaepermeier/r2-revisited>.

4.1 Comparison of Discrete and Exact R2 Values

We start by comparing the exact R2 indicator as computed using our method (see Section 3) with the discretized version found throughout the literature. As a basis for the comparison, we rely on the nondominated points found by evaluating 10^5 solutions on a bi-sphere problem from the bi-objective BBOB [4]. We evaluated the discretized R2 with uniformly distributed weights, and the number of weights ($|W|$) ranging from one to one million. The value of the discretized indicator as well as the approximation error are visualized in Figure 4.

We can see that, in this example, the R2 indicator seems sufficiently well approximated at around 1,000 weights. Still, more weights yield a more accurate approximation: Empirically, there seems to be an exponential relationship between the number of weights chosen and the approximation error. This reflects analyses by [5] on the behavior of the discrete R2 with an increasing number of weights, albeit missing the exact R2 values for comparison.

4.2 Exact R2 Indicator Values

For the exact R2 indicator, we can provide the optimal indicator values for simple solution sets and corresponding test functions. This contributes to a better understanding of the R2 indicator values, as a geometric interpretation like with the hypervolume indicator is not possible.

Nadir and Ideal Points Assuming we have normalized the objective space ((0, 0) being the ideal point and (1, 1) being the nadir point), we can compute the R2 indicator for the worst possible solution within the region of interest $[0, 1] \times [0, 1]$ by inserting the nadir point (1, 1) into the equation. According to the previous results, and with $w^* = 0.5$ to fulfill $w^*y_1 = (1 - w^*)y_2$, we can compute this value as follows:

$$\begin{aligned} R2(\{(1, 1)\}) &= \frac{1}{2}y_2(1 - (1 - w^*)^2) + \frac{1}{2}y_1(1 - (w^*)^2) \\ &= 0.5 \cdot 1(1 - (1 - 0.5)^2) + 0.5 \cdot 1(1 - 0.5^2) \\ &= 0.5 \cdot 0.75 + 0.5 \cdot 0.75 = \mathbf{0.75}. \end{aligned}$$

This result is independent of the particular problem or PF, as it is only dependent on the normalized nadir and ideal points. Analogously, we can derive the R2 value for the ideal point as $R2(\{(0, 0)\}) = \mathbf{0}$, as all utilities equal zero at the ideal point. For comparison, the HV w.r.t. the nadir point as the reference point is $HV(\{(1, 1)\}) = 0$, while the HV of the ideal point is $HV(\{(0, 0)\}) = 1$ in this situation.

Linear Front Let us now consider a linear PF where $y_2 = 1 - y_1$ and $y_1 \in [0, 1]$ with ideal point (0, 0). When computing R2, for each weight vector w , we can find the optimal solution y on the PF, which we can derive as follows:

$$w_1y_1 = w_2y_2 \Rightarrow w_1y_1 = (1 - w_1)(1 - y_1) \Leftrightarrow y_1 = 1 - w_1.$$

Note that when we use this, it does not matter which of the objectives we consider in the R2 computation, as they will always yield the same utility value. Integrating over the weights for this set Y_{1in} , we get:

$$\begin{aligned} R2(Y_{1in}) &= \int_0^1 \min_{y \in Y_{1in}} \{\max(wy_1, (1 - w)y_2)\} dw \\ &= \int_0^1 wy_1 dw = \int_0^1 w(1 - w) dw = \int_0^1 (w - w^2) dw \\ &= \left[\frac{1}{2}w^2 - \frac{1}{3}w^3 \right]_0^1 \\ &= \frac{1}{2} - \frac{1}{3} = \frac{\mathbf{1}}{\mathbf{6}} \approx \mathbf{0.1667}. \end{aligned}$$

Based on this result, we can derive that the optimal R2 indicator value for the DTLZ1 problem [7], which possesses a linear PF with ideal point (0, 0) and nadir point (0.5, 0.5), is $\frac{1}{12} \approx 0.0833$.

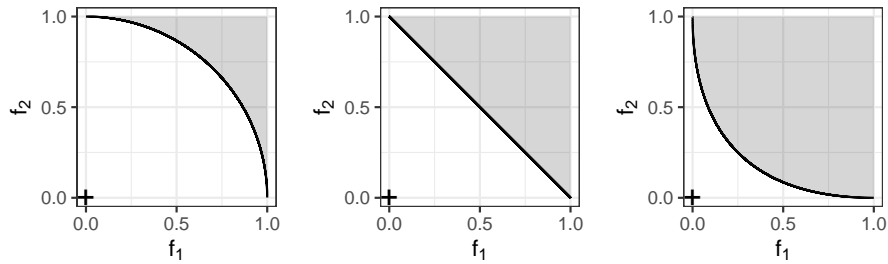


Fig. 5. Schematic illustration of a concave ($\frac{3}{4} < R2 < \frac{1}{6}$), linear ($R2 = \frac{1}{6}$), and convex ($0 < R2 < \frac{1}{6}$) PF, respectively. The ideal point at the origin is denoted by +, and the gray area indicates the dominated area.

Convex and Concave Fronts Additionally, we can derive value ranges for general concave and convex PFs: A concave front Y_{conc} will always achieve worse utility values than a linear function, and a convex front Y_{conv} will always have better utility. Again considering the normalized objective space, a general concave front has an ideal R2 value between the value of the linear front and the nadir point's value, i.e., $\frac{1}{6} < R2(Y_{\text{conc}}) < \frac{3}{4}$. Analogously, a convex front Y_{conv} will always fall between the R2 values of the ideal point and the linear front, i.e., $0 < R2(Y_{\text{conv}}) < \frac{1}{6}$. All cases are illustrated in Figure 5. If none of the discussed conditions apply, the ideal R2 indicator value of the normalized objective space may lie anywhere between 0 and 0.75.

As shown above, exact R2 indicator values can be derived for certain analytical PF shapes. Following the same pattern, that is, resolving $w_1 y_1 = (1 - w_1) y_2$ and integrating the utility function, we can compute the exact indicator values also for more complex PF shapes, albeit in a less straightforward manner. We limit ourselves to reporting the results for simple quadratic PF functions, which correspond to the PFs in Figure 5:

- Convex PF with $y_2 = (1 - \sqrt{y_1})^2$: $\frac{3\pi-8}{16} \approx 0.0890$
- Concave PF with $y_2 = \sqrt{1 - y_1}^2$: $\frac{1}{8} (3\sqrt{2} \sinh^{-1}(1) - 2) \approx 0.2174$

The result for the convex PF applies, e.g., for the classical bi-sphere problem, while the concave PF corresponds to DTLZ2 [7].

To summarize, we can compute exact R2 indicator values for different simple front shapes and individual points. While these values do not seem to have an intuitive (geometric) interpretation, they are rather given meaning by the expected utility to a decision-maker.

5 Conclusion

In this paper, we introduce a procedure to compute the exact R2 indicator value for a given solution set. In contrast to its widely-known and commonly

used discrete counterpart, the exact R2 indicator is not just weakly Pareto-compliant, but a proper Pareto-compliant indicator. This is achieved by foregoing the discretization of the distribution of utility functions usually performed in the calculation of the indicator and taking a continuous, uniform distribution of Tchebycheff utility functions as the basis. Pareto compliance of the R2 indicator with this utility distribution was already described when it was introduced by [10], but missing instructions for its exact calculation. Further, we show how this indicator is implemented efficiently with a running time of $\mathcal{O}(N \log N)$ for bi-objective solution sets of size N . This positions the exact R2 indicator as a promising Pareto-compliant alternative to the hypervolume indicator, especially when a utopian rather than an anti-optimal reference point is naturally available.

We demonstrate the approximation behaviour of the commonly used, discretized R2 indicator in comparison with the exact computation, and provide optimal R2 indicator values for the ideal and nadir points, as well as a linear front in normalized objective space. From this, we derive R2 indicator value ranges for general convex and concave PFs as well.

We expect that the exact R2 indicator offers multiple directions for further theoretical and empirical research. So far, we have only demonstrated how the R2 indicator is computed for bi-objective problems. A natural further research direction pertains to the computation of the indicator for more than two objectives. We do not expect that the R2 indicator will provide a runtime advantage over the hypervolume indicator, however, schemes to approximate it are until now the state-of-the-art in its computation and therefore very accessible compared to HV approximations. We also believe that an incremental variant of the indicator can be designed, which would make it ideal for benchmarking applications, where an indicator should be computed iteratively for the whole archive of solutions.

From a theoretical point of view, we see potential in analyzing the approximation quality of the discretized R2 depending on the number of weights used. This could be particularly interesting for giving quality guarantees for R2 in higher-dimensional objective spaces, where exact indicator computations may become computationally intractable. A deeper theoretically supported analysis of its properties, along the lines of [5], would also be interesting. Further, the effects of different utility functions as well as the integration of (decision-maker) preferences can be examined, as both directions have been studied in detail for the discretized R2 indicator [15]. Finally, connections between the R2 indicator and the integrated preference functional [6,3], a parallel development of an indicator very similar to R2 in the operations research community, should be further investigated, and could yield improvements in understanding the R2 indicator's properties and computation.

Differences and similarities in the preferred distributions between the exact R2 indicator and the hypervolume indicator when applying them in a benchmarking context could present a promising research direction. Likewise, integrating the exact R2 in optimization heuristics, similar to R2-EMOA [14], may be the subject of future studies.

Acknowledgments. The work of Lennart Schäpermeier and Pascal Kerschke was supported by the *Center for Scalable Data Analytics and Artificial Intelligence (ScaDS.AI) Dresden/Leipzig*.

References

1. Audet, C., Bigeon, J., Cartier, D., Le Digabel, S., Salomon, L.: Performance indicators in multiobjective optimization. *European journal of operational research* **292**(2), 397–422 (2021)
2. Beume, N., Fonseca, C.M., López-Ibáñez, M., Paquete, L., Vahrenhold, J.: On the complexity of computing the hypervolume indicator. *IEEE Trans. Evol. Comput.* **13**(5), 1075–1082 (2009). <https://doi.org/10.1109/TEVC.2009.2015575>
3. Bozkurt, B., Fowler, J.W., Gel, E.S., Kim, B., Köksalan, M., Wallenius, J.: Quantitative comparison of approximate solution sets for multicriteria optimization problems with weighted tchebycheff preference function. *Operations research* **58**(3), 650–659 (2010)
4. Brockhoff, D., Auger, A., Hansen, N., Tusar, T.: Using well-understood single-objective functions in multiobjective black-box optimization test suites. *Evol. Comput.* **30**(2), 165–193 (2022). https://doi.org/10.1162/EVC0_A_00298
5. Brockhoff, D., Wagner, T., Trautmann, H.: On the properties of the R2 indicator. In: *Proceedings of the 14th annual conference on Genetic and evolutionary computation*. pp. 465–472 (2012)
6. Carlyle, W.M., Fowler, J.W., Gel, E.S., Kim, B.: Quantitative comparison of approximate solution sets for bi-criteria optimization problems. *Decision Sciences* **34**(1), 63–82 (2003)
7. Deb, K., Thiele, L., Laumanns, M., Zitzler, E.: Scalable test problems for evolutionary multiobjective optimization. In: *Evolutionary multiobjective optimization: theoretical advances and applications*, pp. 105–145. Springer (2005)
8. Grimme, C., Kerschke, P., Aspar, P., Trautmann, H., Preuss, M., Deutz, A.H., Wang, H., Emmerich, M.: Peeking beyond peaks: Challenges and research potentials of continuous multimodal multi-objective optimization. *Computers & Operations Research* **136**, 105489 (2021)
9. Guerreiro, A.P., Fonseca, C.M., Paquete, L.: The hypervolume indicator: Computational problems and algorithms. *ACM Comput. Surv.* **54**(6), 119:1–119:42 (2022). <https://doi.org/10.1145/3453474>
10. Hansen, M.P., Jaskiewicz, A.: Evaluating the quality of approximations to the non-dominated set. IMM, Department of Mathematical Modelling, Technical University of Denmark (1998)
11. Ishibuchi, H., Masuda, H., Tanigaki, Y., Nojima, Y.: Modified distance calculation in generational distance and inverted generational distance. In: *Evolutionary Multi-Criterion Optimization: 8th International Conference, EMO 2015, Guimarães, Portugal, March 29–April 1, 2015. Proceedings, Part II* 8. pp. 110–125. Springer (2015)
12. Mersmann, O.: *emoa: Evolutionary Multiobjective Optimization Algorithms* (2023), <https://CRAN.R-project.org/package=emoa>, R package version 0.5-0.2
13. Miettinen, K.: *Nonlinear multiobjective optimization*, vol. 12. Springer Science & Business Media (1999)
14. Trautmann, H., Wagner, T., Brockhoff, D.: R2-EMOA: Focused multiobjective search using R2-indicator-based selection. In: *Learning and Intelligent Optimization: 7th International Conference, LION 7, Catania, Italy, January 7-11, 2013, Revised Selected Papers* 7. pp. 70–74. Springer (2013)

15. Wagner, T., Trautmann, H., Brockhoff, D.: Preference articulation by means of the R2 indicator. In: *Evolutionary Multi-Criterion Optimization: 7th International Conference, EMO 2013, Sheffield, UK, March 19-22, 2013. Proceedings 7*. pp. 81–95. Springer (2013)
16. Zitzler, E., Knowles, J.D., Thiele, L.: Quality assessment of pareto set approximations. In: Branke, J., Deb, K., Miettinen, K., Slowinski, R. (eds.) *Multiobjective Optimization, Interactive and Evolutionary Approaches* [outcome of Dagstuhl seminars]. *Lecture Notes in Computer Science*, vol. 5252, pp. 373–404. Springer (2008). https://doi.org/10.1007/978-3-540-88908-3_14
17. Zitzler, E., Thiele, L.: Multiobjective optimization using evolutionary algorithms—a comparative case study. In: *International conference on parallel problem solving from nature*. pp. 292–301. Springer (1998)
18. Zitzler, E., Thiele, L., Laumanns, M., Fonseca, C.M., da Fonseca, V.G.: Performance assessment of multiobjective optimizers: an analysis and review. *IEEE Trans. Evol. Comput.* **7**(2), 117–132 (2003). <https://doi.org/10.1109/TEVC.2003.810758>